SEARCHES FOR HIGGS BOSONS

Updated January 2002 by P. Igo-Kemenes
(Physikalisches Institut, Heidelberg, Germany).

I. Introduction

One of the main challenges in high-energy physics is to understand electroweak symmetry breaking and the origin of mass. In the Standard Model (SM) [1], the electroweak interaction is described by a gauge field theory based on the $\mathrm{SU}(2)_L \times \mathrm{U}(1)_Y$ symmetry group. Masses can be introduced by the Higgs mechanism [2]. In its simplest form, which is implemented in the SM, fundamental scalar Higgs fields interact with each other such that they acquire non-zero vacuum expectation values, and the $\mathrm{SU}(2)_L \times \mathrm{U}(1)_Y$ symmetry is spontaneously broken down to the electromagnetic $\mathrm{U}(1)_{EM}$ symmetry. Gauge bosons and fermions obtain their masses by interacting with the vacuum Higgs fields. Associated with this description is the existence of massive scalar particles, Higgs bosons.

The minimal SM requires one Higgs field doublet, and predicts a single neutral Higgs boson, H^0. Beyond the SM, supersymmetric (SUSY) extensions [3] are of interest since they provide a consistent framework for the unification of the gauge interactions at a high energy scale, $\Lambda_{\mathrm{GUT}} \approx 10^{16}$ GeV, and an explanation for the stability of the electroweak energy scale in the presence of quantum corrections (the "scale hierarchy problem"). Moreover, their predictions are compatible with existing high-precision data.

The Minimal Supersymmetric Standard Model (MSSM) (reviewed *e.g.*, in Ref. 4) is the SUSY extension of the SM with minimal new particle content. It introduces two Higgs field doublets, which is the minimal Higgs structure required to keep the theory free of anomalies, and to give masses to all charged fermions. The MSSM is a Two Higgs Doublet Model (2HDM) of "type II," where the neutral component of one field doublet couples to down quarks and charged leptons, while that of the other couples to up quarks only. Assuming CP invariance, the spectrum of MSSM Higgs bosons consists of two CP-even neutral scalars, h^0 and H^0 (h^0 is defined to be the lighter one),

one CP-odd neutral scalar, A^0, and one pair of charged Higgs bosons, $H^\pm$.

Prior to 1989, when the e^+e^- collider LEP at CERN came into operation, the searches for Higgs bosons were sensitive to masses below a few GeV only (see Ref. 5 for a review). From 1989 to 1994 (the LEP1 phase), the LEP collider was operating at a center-of-mass energy $\sqrt{s} \approx M_Z$. After 1994 (the LEP2 phase), the center-of-mass energy increased each year, reaching 208 GeV in the year 2000 before the final shutdown. The combined data of the four LEP experiments, ALEPH, DELPHI, L3, and OPAL, are sensitive to Higgs bosons with masses up to the kinematic limit of the principal production processes, $e^+e^- \to H^0Z^0$ and h^0Z^0, that is, $(\sqrt{s})_{\rm max}$–$M_Z \approx 117$ GeV.

Searches have also been carried out at the Tevatron $p\overline{p}$ collider operating at $\sqrt{s} = 1.8$ TeV. With the currently available data samples, the sensitivity of the two experiments, CDF and DØ, is rather limited, but with increasing sample sizes, the range of sensitivity will eventually exceed the LEP range [6]. Later, the searches will continue at the LHC pp collider, covering masses up to about 1 TeV [7]. If Higgs bosons are indeed discovered, the Higgs mechanism could be studied in great detail at future e^+e^- [8,9] and $\mu^+\mu^-$ colliders [10].

In order to provide an up-to-date review, in some cases recent unpublished documents are also quoted. These are marked by (*) in the reference list, and can be accessed conveniently from the web page of Ref. 11 *("Information for PDG-2002")* . Results of the LEP Higgs Working Group (LHWG), obtained from combining the data of the four LEP experiments, can be accessed from Ref. 11 *("Papers")*. In each case, the LHWG documents list the papers from the individual experiments which have contributed to the combined result.

II. Higgs phenomenology

In this section, we summarize some features of the phenomenology [12,13] which govern the searches for Higgs bosons at LEP and at the Tevatron. Predictions for Higgs boson

masses, as well as production and decay properties, are discussed.

Higgs boson masses

In the SM, the Higgs boson mass, $m_{H^0} = \sqrt{2\lambda}\ v$, is proportional to the vacuum expectation value v of the Higgs field, which is fixed by the Fermi coupling. The quartic Higgs coupling λ, and thus m_{H^0}, is not predicted, but arguments of self-consistency of the theory can be used to place approximate upper and lower bounds on m_{H^0} [14,15].

Since for large Higgs masses the running coupling λ rises with energy, the theory would eventually become non-perturbative. The requirement that in the SM this does not occur below a given energy scale Λ defines an upper bound for the Higgs mass. A lower bound is obtained from the study of quantum corrections to the SM effective potential. The requirement that the electroweak minimum remains an absolute minimum up to a scale Λ (or that the lifetime of the electroweak minimum is large compared to the age of the universe) yields a "vacuum stability" condition which limits m_{H^0} from below.

These theoretical bounds are summarized in Fig. 1. If the SM is to be self-consistent up to $\Lambda_{\rm GUT} \approx 10^{16}$ GeV, there remains only a narrow band from about 130 to 190 GeV for the Higgs mass. Even stronger restrictions are obtained using arguments of naturalness and fine-tuning [16]. The discovery of a Higgs boson with mass below 130 GeV would suggest the onset of new physics at a scale below $\Lambda_{\rm GUT}$, which is predicted, for example, by SUSY models. The dark bands in Fig. 1 represent theoretical uncertainties, with the top quark mass fixed at $m_t = 175$ GeV. For lower values of m_t, compatible with the measurements, the lower bound can be significantly softer.

Indirect experimental bounds for the SM Higgs boson mass are obtained from fits to precision measurements of electroweak observables, primarily from Z^0 decay data, and to the measured top and $W^\pm$ masses. These measurements are sensitive to $\log(m_{H^0})$ through radiative corrections. The best fit value is $m_{H^0} = 88^{+53}_{-35}$ GeV, or m_{H^0} <196 GeV at the 95% confidence

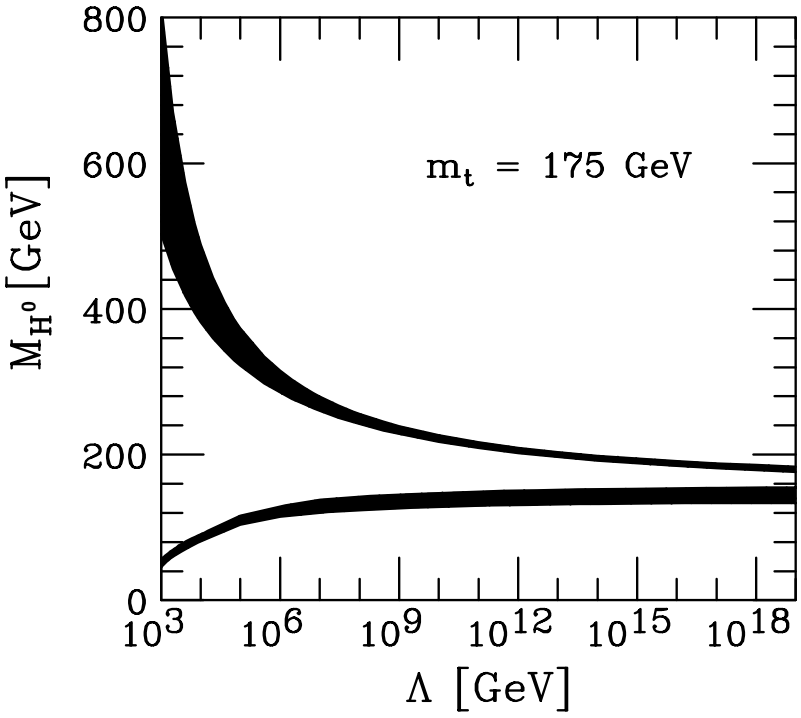

Figure 1: Bounds on the Higgs boson mass based on arguments of self-consistency of the SM (from Ref. 15). Λ denotes the energy scale at which the SM would become non-perturbative or the electroweak potential unstable.

level (CL) [17], which is still consistent with the SM being valid up to the GUT scale.

In the MSSM and at tree level, only two parameters are required (beyond known parameters of the SM fermion and gauge sectors) to fix all Higgs boson masses and couplings. A convenient choice is the mass m_{A^0} of the CP-odd scalar A^0, and the ratio $\tan\beta{=}v_2/v_1$ of the vacuum expectation values associated to the neutral components of the two Higgs fields (v_2 and v_1 couple to up and down fermions, respectively). Often the mixing angle α is used, which diagonalises the CP-even Higgs mass matrix; α can also be expressed in terms of m_{A^0} and $\tan\beta$. The following ordering of masses is valid at tree level: $m_{h^0} < (M_Z,\ m_{A^0}) < m_{H^0}$ and $M_W < m_{H^\pm}$. These relations are modified by radiative corrections [18,19].

The largest contribution arises from the incomplete cancelation between top and scalar-top (stop) loops. The corrections affect mainly the masses and decay branching ratios in the neutral Higgs sector; they depend strongly on the top quark mass ($\sim m_t^4$) and logarithmically on the stop masses, and involve a detailed parameterization of soft SUSY breaking and the mixing between the SUSY partners of left- and right-handed top quarks (stop mixing).

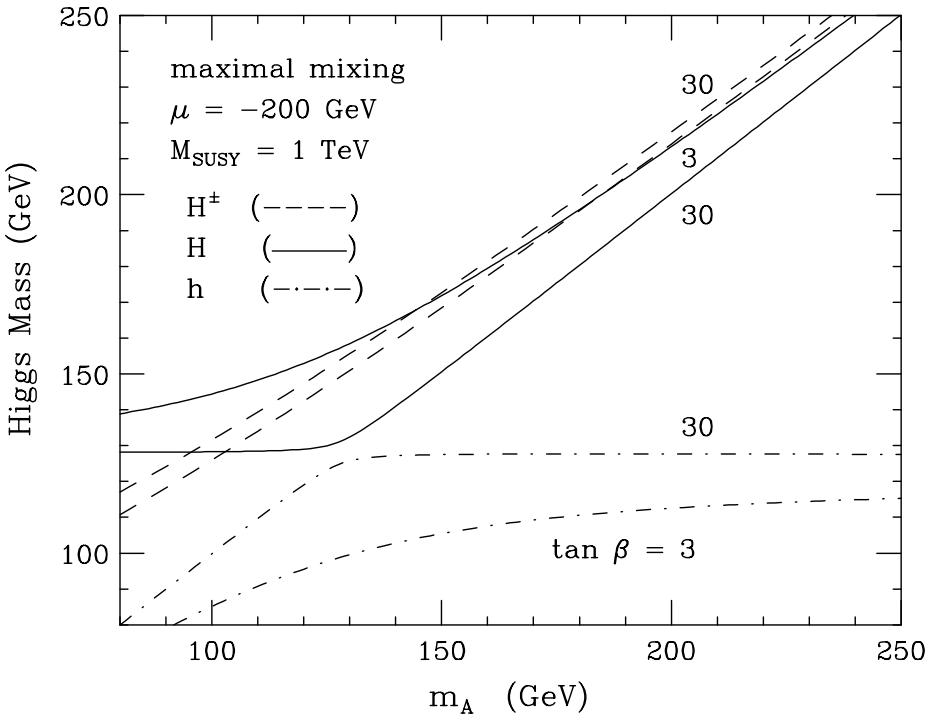

Figure 2: Higgs boson masses in the MSSM after radiative corrections, as a function of m_{A^0}, for $\tan\beta = 3$ and 30 (from Ref. 6).

The Higgs boson masses, after radiative corrections, are displayed in Fig. 2 for two representative values of $\tan\beta$ within the range from 1 to $\approx m_t/m_b$, which is preferred in some grand unification schemes [20], and in the simplest models of SUSY breaking.

Higgs boson production

The principal mechanism for producing the SM Higgs particle at LEP is Higgs-strahlung in the s-channel [21], $e^+e^- \to H^0Z^0$, where a Higgs boson is radiated off an intermediate Z^0 boson. The Z^0 boson in the final state is either virtual (LEP1) or on mass shell (LEP2). The cross section [22], $\sigma^{\rm SM}_{HZ}$, is shown in Fig. 3, together with those of the dominant SM background processes, $e^+e^- \to$ fermion pairs, W^+W^-, and Z^0Z^0.

The SM Higgs boson can also be produced by W^+W^- fusion in the t-channel [23], $e^+e^- \to \overline{\nu}_e\nu_e H^0$, but at LEP energies this process has a small contribution to the cross section, except for masses which cannot be reached by the Higgs-strahlung process. The contribution from Z^0Z^0 fusion, $e^+e^- \to e^+e^-H^0$, is insignificant.

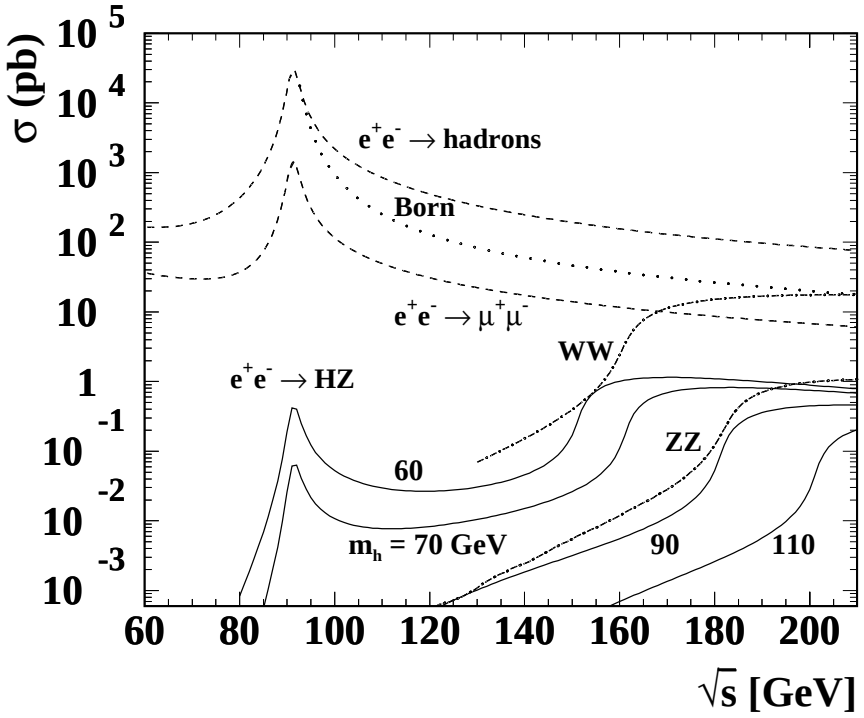

Figure 3: Cross sections, as a function of $\sqrt{s}$, for the Higgs-strahlung process in the SM for fixed values of m_{H^0} (full lines), and for other SM processes which contribute to the background.

In the 2HDM of "type II," of which the MSSM is a particular realization with SUSY, the main production mechanisms of the neutral Higgs bosons h^0 and A^0 are the Higgs-strahlung process $e^+e^- \to h^0Z^0$, and the pair production process $e^+e^- \to h^0A^0$. Fusion processes play a marginal role at LEP. The cross sections for Higgs-strahlung and pair production can be expressed in terms of the SM cross section $\sigma_{HZ}^{\rm SM}$, and the angles α and β introduced before:

$$\sigma_{h^0Z^0} = \sin^2(\beta-\alpha)\ \sigma_{HZ}^{\rm SM} \tag{1}$$

$$\sigma_{h^0A^0} = \cos^2(\beta-\alpha)\overline{\lambda}\ \sigma_{HZ}^{\rm SM}\ , \tag{2}$$

with the kinematic factor $\overline{\lambda} = \lambda_{A^0h^0}^{3/2} / \left[\lambda_{Z^0h^0}^{1/2}(12M_Z^2/s + \lambda_{Z^0h^0})\right]$ and $\lambda_{ij} = \left[1-(m_i+m_j)^2/s\right]\left[1-(m_i-m_j)^2/s\right]$. The two cross sections have complementary suppression factors $\sin^2(\beta-\alpha)$ and $\cos^2(\beta-\alpha)$. In the MSSM, the process $e^+e^- \to h^0Z^0$ has the larger cross section at small $\tan\beta$, while at large $\tan\beta$ it is $e^+e^- \to h^0A^0$, unless suppressed kinematically.

Charged Higgs bosons are expected to be produced at LEP in pairs [12,24], $e^+e^- \to H^+H^-$, and the cross section is fixed at tree level by the mass $m_{H^\pm}$.

At the Tevatron, the dominant production mechanism for the SM Higgs boson is gluon fusion, $gg \to H^0$ [25], but the mechanism with the most promising detection possibilities is the production in association with a vector boson, $p\overline{p} \to H^0V$ ($V \equiv W^\pm,\ Z^0$), where the leptonic decays of the vector boson can be exploited for triggering [6]. The cross sections for this and other Higgs production processes are shown in Fig. 4.

Over most of the MSSM parameter space, one of the CP-even Higgs bosons (h^0 or H^0) couples to the vector bosons with SM-like strength. Like in the SM case, the associated production, $p\overline{p} \to (h^0$ or $H^0)V$ (with $V \equiv W^\pm,\ Z^0$), is the most promising search mechanism. The gluon fusion processes, $gg \to h^0$, H^0, A^0, are dominant, but in this case, only the Higgs to $\tau^+\tau^-$ decay mode is promising, since the main $b\overline{b}$ decay mode is overwhelmed by QCD background.

Charged Higgs bosons with mass less than $m_t - m_b$ can be produced at the Tevatron in the decay of the top quark,

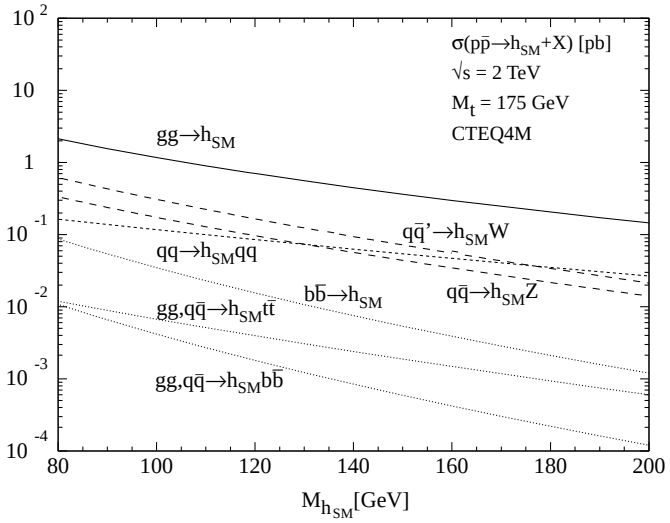

Figure 4: Cross sections (in units of pb), as a function of the mass, for the most relevant SM Higgs production processes in $p\overline{p}$ collisions at $\sqrt{s} = 2$ TeV (from Ref. 6).

$t \to H^+ b$. This process can compete with the SM decay, $t \to W^+ b$, depending on the value of $\tan\beta$. Assuming that no other decay process contributes, the cross section for charged Higgs production in top quark decay is related to the $t\overline{t}$ cross section and the $t^+ \to W^+ b$ branching ratio:

$$\sigma(p\overline{p} \to H^{\pm}\text{+X}) = \left[1 - \text{BR}(t \to W^+ b)^2\right] \;\; \sigma(p\overline{p} \to t\overline{t}\text{+X}). \quad (3)$$

Higgs boson decays

The most relevant decays of the SM Higgs particle [22,24] are summarized in Fig. 5. For masses below about 140 GeV, decays to fermion anti-fermion pairs dominate, and $H^0 \to b\overline{b}$ has the largest branching ratio. Decays to $\tau^+\tau^-$, $c\overline{c}$, and gluon pairs (via loops) contribute less than 10%. For such low masses, the decay width is less than 10 MeV. For larger masses, the W^+W^- and Z^0Z^0 final states dominate and the

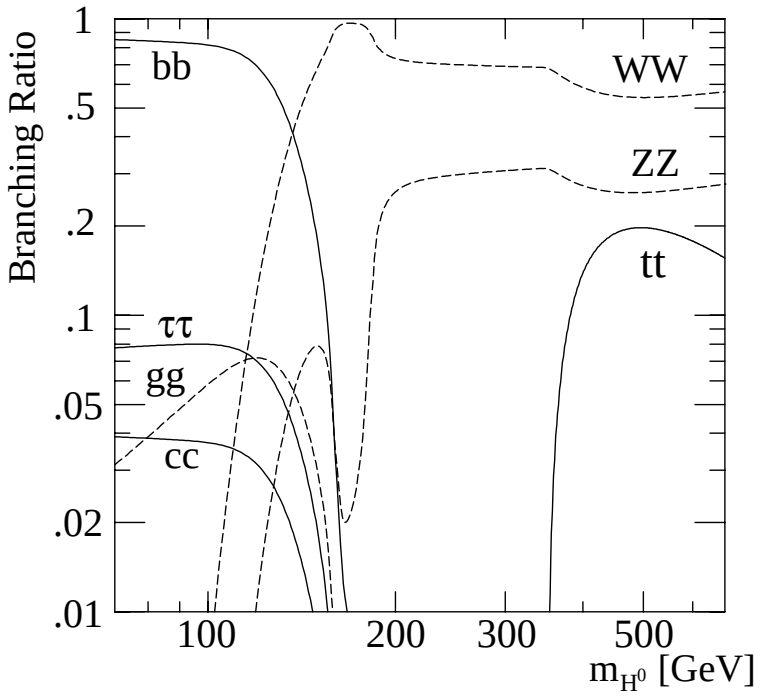

Figure 5: Branching ratios for the main decay modes of the SM Higgs boson (from Ref. 8).

decay width rises rapidly with mass, reaching about 1 GeV for $m_{H^0} = 200$ GeV, and 100 GeV for $m_{H^0} = 500$ GeV.

In the 2HDM of "type II," and thus in the MSSM, the couplings of the neutral Higgs bosons to quarks, leptons, and gauge bosons are modified with respect to the SM Higgs couplings by factors which depend upon the angles α and β. These factors, valid at tree level, are summarized in Table 1.

Table 1: Factors relating the 2HDM Higgs couplings to the couplings in the SM.

	"Up" fermions	"Down" fermions	Vector bosons
SM Higgs:	1	1	1
2HDM h^0 :	$\cos\alpha/\sin\beta$	$-\sin\alpha/\cos\beta$	$\sin(\beta-\alpha)$
H^0 :	$\sin\alpha/\sin\beta$	$\cos\alpha/\cos\beta$	$\cos(\beta-\alpha)$
A^0 :	$1/\tan\beta$	$\tan\beta$	0

The following features are relevant to decays of neutral Higgs bosons in the MSSM. The h^0 boson will decay mainly to fermion pairs, since the mass is smaller than about 130 GeV. The A^0 boson also decays predominantly to fermion pairs, independently of its mass, since its coupling to vector bosons is zero at leading order (see Table 1). For $\tan\beta > 1$, decays to $b\overline{b}$ and $\tau^+\tau^-$ pairs are preferred, with branching ratios of about 90% and 8%, respectively, while the decays to $c\overline{c}$ and gluon pairs are suppressed. Decays to $c\overline{c}$ may become important for $\tan\beta < 1$. The decay $h^0 \to A^0A^0$ may become dominant if it is kinematically allowed. Other possible decays go to SUSY particles such as sfermions, charginos or neutralinos, which may lead to invisible or barely visible final states. The branching fractions for such decays can be dominant in parts of the MSSM parameter space, thus requiring special search strategies.

The charged Higgs bosons of the 2HDM decay mainly via $H^+ \to \tau^+\nu_\tau$ if $\tan\beta$ is large. For small $\tan\beta$, the decay to $c\overline{s}$ is dominant at low mass, and the decay to $H^+ \to t^*\overline{b} \to W^+b\overline{b}$ is dominant for $m_{H^\pm}$ larger than about 130 GeV [26].

III. Searches for the SM Higgs boson

During the LEP1 phase, the experiments ALEPH, DELPHI, L3, and OPAL analyzed over 17 million Z^0 decays. They have set lower bounds of approximately 65 GeV on the mass of the SM Higgs boson, and of about 45 GeV on the masses of the h^0, A^0 (valid for $\tan\beta > 1$), and $H^\pm$ bosons [27]. Substantial data samples have also been collected at LEP2 energies, including more than 40,000 $e^+e^- \to W^+W^-$ events. At LEP2, the composition of the background is more complex than at LEP1 (see Fig. 3), due to the additional SM processes $e^+e^- \to W^+W^-$ and Z^0Z^0. These have kinematic properties similar to the signal, especially for $m_{H^0} \sim M_W$ and M_Z, but since at LEP2 the Z^0 boson is on mass shell, constrained kinematic fits yield sufficient separation power. Furthermore, the four collaborations have considerably upgraded their b-tagging capabilities for LEP2. Jets with b flavor (such as from Higgs boson decays) are recognized by the presence of secondary decay vertices, or tracks with large impact parameters identified

by means of high-precision silicon microvertex detectors. Other useful indicators for b flavor are high-p_T leptons from $b \to c\ell^-\overline{\nu}_\ell$ decays ($\ell = e, \mu$) and several jet properties, all of which are combined using likelihood or neural network techniques.

The following final states provide good sensitivity for the SM Higgs boson.

(a) The most abundant, four-jet topology is produced in the $e^+e^- \to (H^0 \to b\overline{b})(Z^0 \to q\overline{q})$ process, and occurs with a branching ratio of about 60%. The invariant mass of two jets is close to M_Z, while the other two jets contain b flavor. The Higgs boson mass is reconstructed with a typical resolution of 2.5 GeV.

(b) The missing energy topology is produced mainly in the $e^+e^- \to (H^0 \to b\overline{b})(Z^0 \to \nu\overline{\nu})$ process, and occurs with a branching ratio of 17%. The signal has two b jets, substantial missing transverse momentum, and missing mass compatible with M_Z. The reconstruction of the Higgs boson mass is achieved with a typical "central" resolution of 3 GeV, but the distribution has pronounced tails. A similar event topology also occurs in the W^+W^- fusion process leading to $b\overline{b}\nu_e\overline{\nu}_e$.

(c) In the leptonic final states, $e^+e^- \to (H^0 \to b\overline{b})(Z^0 \to e^+e^-, \mu^+\mu^-)$, the two leptons reconstruct to M_Z, and the two jets have b flavor. Although the branching ratio is small (only about 6%), this channel adds to the overall search sensitivity since it has low background and good mass resolution, typically 1.5 GeV, if the Higgs boson mass is taken to be the mass recoiling against the reconstructed Z^0 boson.

(d) Final states with tau leptons are produced in the processes $e^+e^- \to (H^0 \to \tau^+\tau^-)(Z^0 \to q\overline{q})$ and $(H^0 \to q\overline{q})(Z^0 \to \tau^+\tau^-)$. They occur with a branching ratio of about 10% in total.

At LEP1, only the missing energy and leptonic final states could be used in the search for the SM Higgs boson, because of prohibitive backgrounds in the other channels. At LEP2, however, all search topologies are included.

The overall sensitivity of the searches is improved by combining statistically the data of the four LEP experiments in different decay channels, and at different LEP energies [28].

After preselection, the combined data configuration (distribution in several global, discriminating variables) is compared in a frequentist approach to Monte Carlo configurations for two hypotheses: the background (b) hypothesis, and the signal + background ($s + b$) hypothesis, where Higgs bosons are assumed to be produced according to the model under consideration: in the case of the SM, the Higgs couplings are fully defined by the hypothesized Higgs boson mass ("test mass") m_H, while in the MSSM and other cases, the model may be defined by a set of parameters. The ratio $Q = \mathcal{L}_{s+b}/\mathcal{L}_b$ of the corresponding likelihoods is used as test statistic to position the observed data configuration between the b and $s + b$ cases. The predicted, normalized distributions of Q (probability density functions) are integrated to obtain the probabilities $1 - \mathrm{CL}_b = 1 - \mathcal{P}_b(Q \leq Q_{\mathrm{observed}})$ and $\mathrm{CL}_{s+b} = \mathcal{P}_{s+b}(Q \leq Q_{\mathrm{observed}})$, which measure the compatibility of the observed data configuration with the two hypotheses.

The searches carried out at LEP prior to the year 2000, and their successive combinations [29], did not reveal any evidence for the production of an SM Higgs boson. In the data of the year 2000, mostly with $\sqrt{s} > 205$ GeV, ALEPH reported an excess of about three-standard deviations beyond the SM background [30], arising mainly from a few four-jet candidates with clean b tags, and kinematic properties suggesting a SM Higgs boson with mass in the vicinity of 115 GeV. The data of DELPHI, L3, and OPAL show no evidence for such an excess, but do not, however, exclude a 115 GeV Higgs boson (see Ref. 31 for the individual publications). When the data of the four experiments are combined [32], the significance decreases to about two standard deviations.

Figure 6 shows the test statistic $-2 \ln Q$ for the ALEPH data and for the LEP data combined. In the LEP data, the minimum is at 115.6 GeV, defining the most likely value for the mass. From the probability density functions for $m_H = 115.6$ GeV, one calculates $1 - \mathrm{CL}_b = 3.4\%$ for the background hypothesis. With $\mathrm{CL}_{s+b} = 0.44$, the observed data configuration is well compatible with the signal + background hypothesis. From the same combination, a 95% CL lower bound of 114.1 GeV is

obtained for the mass. Note that these LEP-combined results are based on a preliminary analysis of ALEPH, DELPHI, and OPAL data, and the final analysis of the L3 data.

At the Tevatron, the results of the CDF [33] and DØ [34] collaborations are currently based on the Run I data samples of about 100 pb^{-1} each. The searches concentrate on the associated production of a Higgs boson with a vector boson, $p\overline{p} \to VH^0$ ($V \equiv Z^0$, $W^\pm$), where the vector boson decays into the leptonic channels $W^\pm \to \ell^\pm\nu$ and $Z^0 \to \ell^+\ell^-$ ($\ell \equiv e,\ \mu$). CDF also considers hadronic decays, and DØ includes the $Z^0 \to \nu\overline{\nu}$ channel. The Higgs boson is assumed to decay into $b\overline{b}$, which is the dominant channel below about 140 GeV mass. Both CDF and DØ have the capability to tag b jets using high-p_T leptons from the $b \to c\ell^-\overline{\nu}$ decay; in the case of CDF, the b tag is made more effective by detecting secondary decay vertices in their silicon microvertex detector. The main source of background is from QCD processes with genuine $b\overline{b}$ pairs.

The current data samples are too small for a discovery, but allow model-independent upper bounds to be set on the cross section for Higgs-like event topologies. These bounds are currently higher by an order of magnitude than the SM predictions; however, Run II started in the year 2001, and with the projected data samples in excess of 10 fb^{-1} per experiment, the search sensitivity will increase considerably.

IV. Searches for neutral MSSM Higgs bosons

The searches at LEP address the Higgs-strahlung process $e^+e^- \to h^0Z^0$, and the pair production process $e^+e^- \to h^0A^0$, exploiting the complementarity of the cross sections expressed in Equations (1) and (2). The results for h^0Z^0 are obtained by re-interpreting the SM Higgs searches, taking into account the reduction of the cross section due to the MSSM factor $\sin^2(\beta-\alpha)$. The results for h^0A^0 are obtained from specific searches for $(b\overline{b})(b\overline{b})$, and $\tau^+\tau^-q\overline{q}$ final states (the $\tau^+\tau^-$ pair may originate from the decay of h^0 or A^0).

The presence of h^0 and/or A^0 is tested in a constrained MSSM model where universal soft SUSY breaking masses, M_{SUSY} and M_2, are assumed for sfermions and SU(2)×U(1)

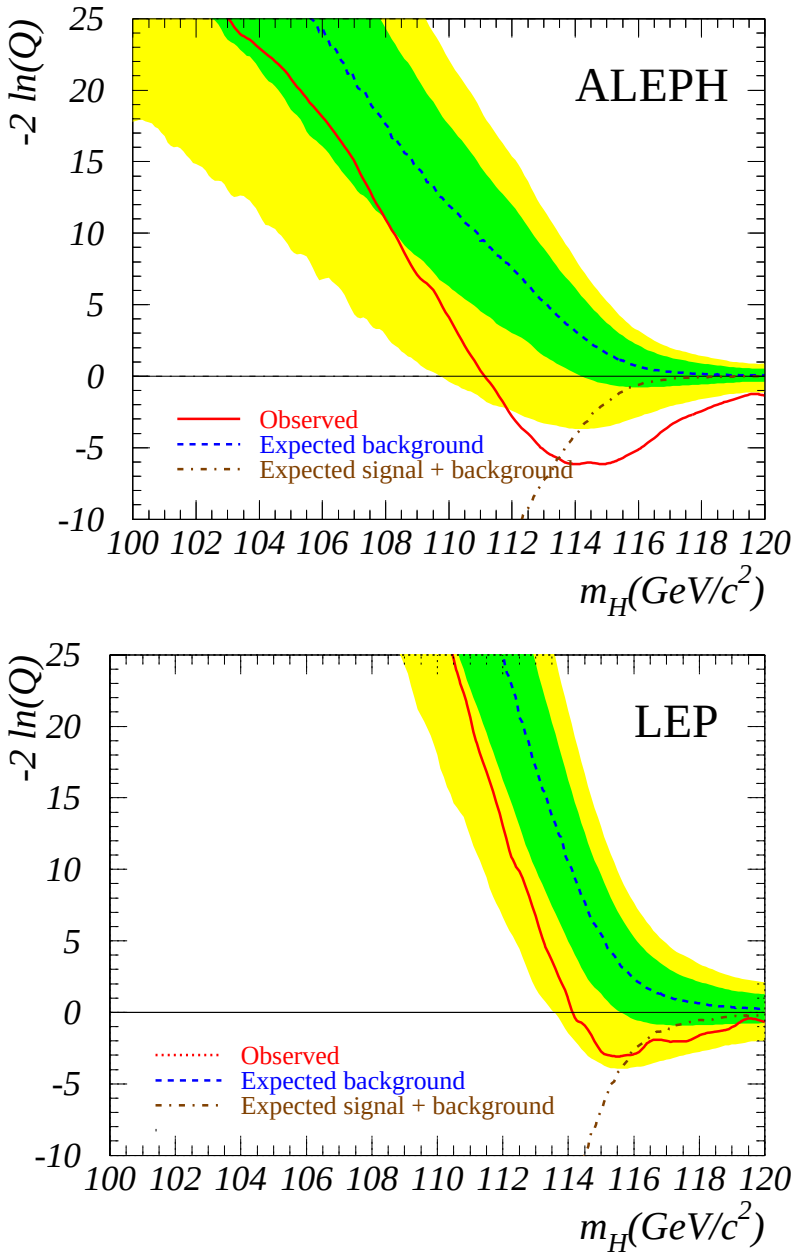

Figure 6: Observed (solid line), and expected behaviors of the test statistic $-2\ln Q$ for the background (dashed line), and the signal + background hypothesis (dash-dotted line), as a function of the test mass m_H. Upper: ALEPH data alone; lower: LEP data combined [32]. The dark- and light-shaded bands represent one and two standard deviation bands about the background expectation.

gauginos, respectively, at the electroweak scale. Further parameters are m_{A^0}, $\tan\beta$, the Higgs mixing parameter μ, and the trilinear Higgs-fermion coupling A. Most results assume the current experimental top quark mass of 174.3 GeV [35]. Furthermore, the gluino mass, which affects the results at the two-loop level, is fixed at 800 GeV. The Higgs decay width is taken to be small compared to the mass resolution, which is a valid assumption for $\tan\beta$ less than about 50.

Although general parameter scans have been carried out [36], most interpretations are limited to specific "benchmark" scenarios [19] where some of the parameters are fixed: $M_{\rm SUSY} =$ 1 TeV, $M_2 = 200$ GeV, and $\mu = -200$ GeV. In the *no-mixing* benchmark scenario, stop mixing is put to zero by choosing $X_t \equiv A - \mu\cot\beta = 0$. The m_{h^0}-max benchmark scenario is designed to maximize m_{h^0} by choosing $X_t = 2M_{\rm SUSY}$. This scenario yields the most conservative exclusion limits, in particular, regarding the value of $\tan\beta$.

The combined LEP limits in the MSSM parameter space [37] are shown in Fig. 7 for the m_{h^0}*-max* scenario (in the *no-mixing* scenario, the unexcluded region is much smaller). The current 95% CL mass bounds are: $m_{h^0} >$91.0 GeV, $m_{A^0} >$91.9 GeV. Furthermore, values of $\tan\beta$ from 0.5 to 2.4 are excluded, but this exclusion can be smaller if, for example, the top mass turns out to be higher than assumed, or $\mathcal{O}(\alpha_t^2 m_t^2)$ two-loop corrections to $m_{h^0}^2$ are included in the model calculation.

The CDF experiment has searched for the Yukawa process $p\overline{p} \to b\overline{b}\ \phi \to b\overline{b}b\overline{b}$ [38], where a Higgs particle ($\phi \equiv h^0$, H^0, A^0) is radiated off a b quark and decays to $b\overline{b}$. This process is enhanced in the MSSM at large $\tan\beta$, where the Yukawa coupling to b quarks is large. The domains excluded by CDF are indicated in Fig. 7, along with the limits from LEP.

V. Searches for charged Higgs bosons

While in the MSSM the mass of the charged Higgs boson is restricted essentially to $m_{H^\pm} > M_W$, such a restriction does not exist in the 2HDM. The searches conducted at LEP and at the Tevatron are, therefore, interpreted primarily in the 2HDM of "type II."

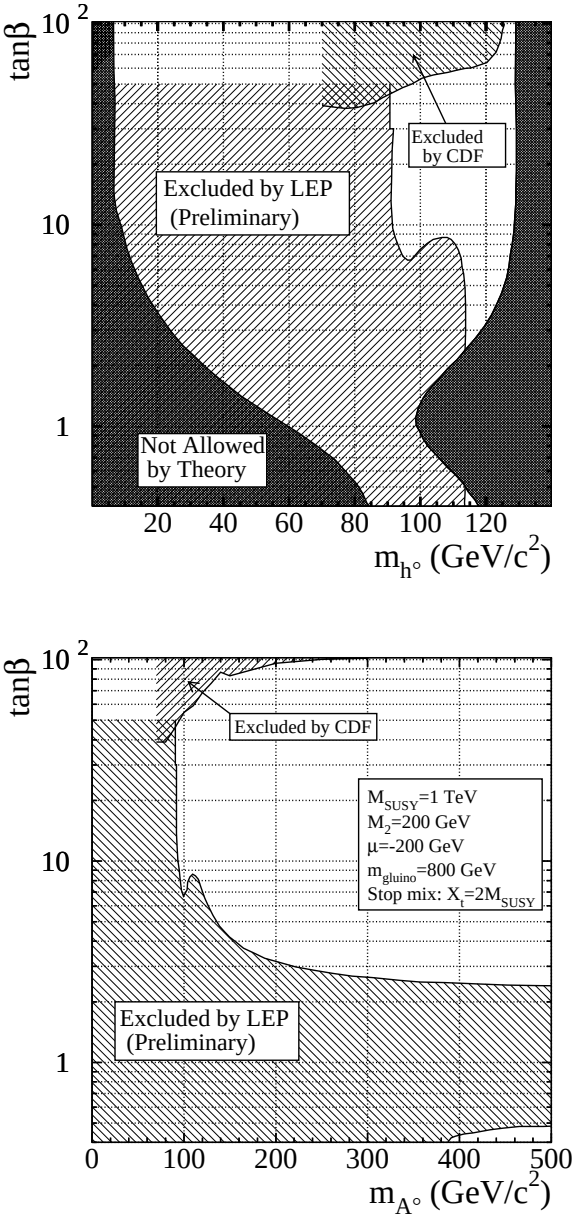

Figure 7: The 95% CL bounds on m_{h^0}, m_{A^0}, and $\tan\beta$ for the m_{h^0}-max benchmark scenario, from LEP [37]. The exclusions at large $\tan\beta$ from CDF [38] are also indicated.

At LEP, charged Higgs bosons are expected to be produced in the process $e^+e^- \to H^+H^-$, and to decay via $H^+ \to c\overline{s}$ and $\tau^+\nu$. While it is assumed that these two channels fully

exhaust the decay width, the relative branching ratio is left free. The following three final states are therefore considered: $(c\overline{s})(\overline{c}s)$, $(\tau^+\nu_\tau)(\tau^-\overline{\nu}_\tau)$, and $(c\overline{s})(\tau^-\overline{\nu}_\tau)+(\overline{c}s)(\tau^+\nu_\tau)$. At LEP2 energies, the sensitivity is limited to masses less than M_W by the background from $e^+e^- \to W^+W^-$. The data of the four LEP experiments have been combined, resulting in a general mass bound of $m_{H^\pm} >$78.6 GeV (95% CL) [39], which is independent of the branching ratio BR($H^+ \to \tau^+\nu$).

The searches at the Tevatron look for charged Higgs bosons in the decay of the top quark, $t \to bH^+$. While the SM requires the top quark to decay almost exclusively via $t \to bW^+$, in the 2HDM the process $t \to bH^+$ may compete if $m_{H^+} < m_t - m_b$, and if $\tan\beta$ is either larger than 30 or less than one. The DØ collaboration has adopted an indirect "disappearance technique" optimized for the detection of $t \to bW^+$, and a direct search for $t \to bH^+ \to b\tau^+\nu_\tau$ [40]. CDF has reported on the direct search for $t \to bH^+$ [41], and on an indirect approach [42] in which the rate of dileptons and lepton+jets in top quark decays is compared to the SM prediction. Both collaborations assume that the H^+ decays into three channels: (i) $c\overline{s}$, which is dominant at low $\tan\beta$ and small $m_{H^\pm}$, (ii) $t^*\overline{b} \to W^+b\overline{b}$, dominant at low $\tan\beta$ and for $m_{H^\pm} \approx m_t + m_b$, and (iii) $\tau^+\nu_\tau$, dominant at high $\tan\beta$. The results from the Tevatron are summarized in Fig. 8, together with the exclusion obtained at LEP. The Tevatron limits are subject to potentially large theoretical uncertainties [43].

Indirect limits in the ($m_{H^\pm}$, $\tan\beta$) plane can be derived by comparing the measured rate of the flavor-changing neutral-current process $b \to s\gamma$ to the SM prediction. In the SM, this process is mediated by virtual $W^\pm$ exchange, and gives rise to a branching ratio of $(3.60 \pm\ 0.30) \times 10^{-4}$, according to a recent evaluation [44]. In the 2HDM of "type II," the branching ratio is altered by contributions from charged Higgs bosons [45]. The current experimental value, $(3.23 \pm\ 0.42) \times 10^{-4}$ [44], obtained from combining the measurements of CLEO, BELLE, and ALEPH [46], is in agreement with the SM prediction. From the comparison, the bound $m_{H^\pm} >$316 GeV (95% CL) is obtained, which is much stronger than the current bounds from direct

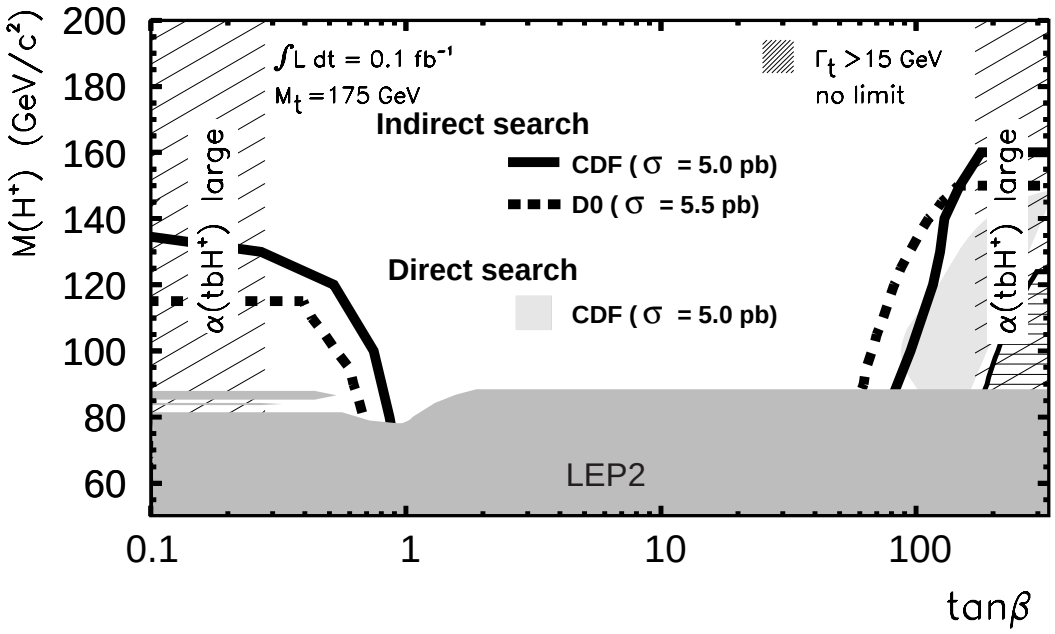

Figure 8: Summary of the 95% CL exclusions in the (m_{H^+}, $\tan\beta$) plane from DØ [40] and CDF [41], using various indirect and direct observation techniques (the regions below the curves are excluded). The two experiments use slightly different theoretical $t\bar{t}$ cross sections, as indicated. The dashed domains at extreme values of $\tan\beta$ are not considered in these searches, since there the tbH^+ coupling becomes large, and perturbative calculations do not apply. The dark region labeled LEP2 is excluded by LEP [39].

searches. However, these indirect bounds are model-dependent and may be invalidated, for example, by sparticle loops or anomalous couplings. Other, less stringent, indirect bounds are obtained from interpretations of measured $b \to \tau^- \nu_\tau$X rates and tau lepton decay properties at LEP [47].

VI. Model extensions

(a) Most of the searches for the processes $e^+e^- \to h^0 Z^0$ and $h^0 A^0$, which have been addressed in Section IV, rely on the experimental signature of Higgs bosons decaying into $b\bar{b}$. While

this assumption is valid over large parts of the MSSM parameter space, in the 2HDM, the h^0 and A^0 decaying to non-$b\overline{b}$ final states may be strongly enhanced. Recently flavor-independent searches have been carried out by the LEP experiments which do not apply b-tagging requirements [48]. In conjunction with the earlier b-flavor sensitive searches, large domains of the general 2HDM parameter space of "type II" could be excluded [49].

(b) The neutral Higgs bosons h^0 and A^0 can also be produced by Yukawa processes $e^+e^- \to f\overline{f}h^0$ and $f\overline{f}A^0$, where these are radiated off a massive fermion ($f \equiv$ b or $\tau^\pm$). These processes can be dominant in regions of the 2HDM space, where the "standard" processes, $e^+e^- \to h^0Z^0$ and h^0A^0, are suppressed. The corresponding enhancement factors (ratios of the 2HDM $f\overline{f}h^0$ and $f\overline{f}A^0$ couplings to the SM $f\overline{f}H^0$ coupling) are $\sin\alpha/\cos\beta$ and $\tan\beta$, respectively. The LEP data have been analyzed, searching specifically for $b\overline{b}b\overline{b}$, $b\overline{b}\tau^+\tau^-$, and $\tau^+\tau^-\tau^+\tau^-$ final states [50]. Regions of low mass and high enhancement factors are excluded by these searches. The CDF search for the analogous $pp \to b\overline{b}$ X process [38] has already been discussed (see Fig. 7).

(c) Higgs bosons with double electric charge, $H^{\pm\pm}$, are predicted by several extensions of the SM, for example, with additional triplet scalar fields or left-right symmetric models [12,51]. OPAL has searched for the process $Z^0 \to H^{++}H^{--}$ with four prompt electrons or muons in the final state, and obtained model-dependent lower bounds in the vicinity of 93 GeV for the mass [52].

(d) The addition of a singlet scalar field to the MSSM [53] gives rise to two additional neutral scalars, one CP-even and one CP-odd. The radiative corrections to the masses are similar to those in the MSSM, and arguments of perturbative continuation to the GUT scale lead to an upper bound of about 135-140 GeV for the mass of the lightest neutral CP-even scalar. DELPHI have reinterpreted their searches for neutral Higgs bosons to constrain such models [54].

(e) Decays into invisible (weakly interacting neutral) particles may occur, for example, in the MSSM, if the Higgs bosons decay to pairs of neutralinos. In a different context,

Higgs bosons might also decay into pairs of massless Goldstone bosons or Majorons [55]. In the process $e^+e^- \to h^0 Z^0$, the mass of the invisible Higgs boson can be inferred from the reconstructed Z^0 boson, using the beam energy constraint. The LEP results have recently been combined, and yield a 95% CL lower bound of 114.4 GeV for the mass of a Higgs boson, with SM production rate and decaying exclusively into invisible final states [56].

(f) Photonic final states from the processes $e^+e^- \to Z^0/\gamma^* \to H^0\gamma$ and from $H^0 \to \gamma\gamma$ do not occur in the SM at tree level, but may be present with a low rate due to $W^\pm$ and top quark loops [57]. Additional loops, for example, from SUSY particles, would increase the rates only slightly [58], but models with anomalous couplings predict enhancements by orders of magnitude. Searches for the processes $e^+e^- \to (H^0 \to b\overline{b})\gamma$, $(H^0 \to \gamma\gamma)q\overline{q}$, and $(H^0 \to \gamma\gamma)\gamma$ have been used to set model-independent limits on such anomalous couplings. They were also used to constrain very specific models leading to an enhanced $H^0 \to \gamma\gamma$ rate, such as the "fermiophobic" 2HDM of "type I" [59], where all fermions couple to the same Higgs field component, and the fermionic decays can thus be suppressed simultaneously by appropriate parameter choices. The searches at LEP have recently been combined [60], and exclude a fermiophobic Higgs boson with mass less than 108.2 GeV (95% CL). Limits of about 80 GeV are obtained at the Tevatron [61].

VII. Prospects

The LEP collider stopped producing data in November 2000. At the Tevatron, Run II started in 2001. Performance studies provide motivation for collecting data samples in excess of 10 fb^{-1} per experiment, which will extend the combined sensitivity of CDF and DØ for the SM Higgs boson search beyond the LEP reach, and allow large domains in the MSSM parameter space to be investigated [6].

The Large Hadron Collider (LHC) should deliver proton-proton collisions at 14 TeV in the year 2007. The ATLAS and CMS detectors have been optimized for Higgs boson searches [7]. The discovery of the SM Higgs boson will be possible over the

mass range between 100 GeV and 1 TeV. This broad range is covered by a variety of production and decay processes. The LHC experiments will provide full coverage of the MSSM parameter space by direct searches for the h^0, H^0, A^0, and $H^\pm$ bosons, and by detecting the h^0 boson in cascade decays of SUSY particles. The discovery of several Higgs bosons is possible over extended domains of the parameter space. Decay branching fractions can be determined and masses measured with statistical accuracies between 10^{-3} (at 400 GeV mass) and 10^{-2} (at 700 GeV mass).

A high-energy e^+e^- linear collider could be realized after the year 2010, running initially at energies up to 500 GeV, and at 1 TeV or more at a later stage [9]. One of the prime goals would be to extend the precision measurements typical of e^+e^- colliders to the Higgs sector. At such a collider, the Higgs couplings to fermions and vector bosons can be measured with precisions of a few percent. The MSSM parameters can be studied in great detail. At the highest collider energies and luminosities, the self-coupling of the Higgs fields can be studied directly through final states with two Higgs bosons [62].

At a future $\mu^+\mu^-$ collider, the Higgs bosons can be generated as s-channel resonances [10]. Mass measurements with precisions of a few MeV would be possible, and the widths could be obtained directly from Breit-Wigner scans. The heavy CP-even and CP-odd bosons H^0 and A^0, degenerate over most of the MSSM parameter space, could be disentangled experimentally.

Finally, if Higgs bosons are not discovered at the TeV scale, both the LHC and the future lepton colliders will be in a position to test alternative theories of electroweak symmetry breaking, such as those with strongly interacting vector bosons [63] expected in theories with dynamical symmetry breaking [64].

References

1. S.L. Glashow, Nucl. Phys. **20**, 579 (1961);
   S. Weinberg, Phys. Rev. Lett. **19**, 1264 (1967);
   A. Salam, *Elementary Particle Theory*, ed. N. Svartholm, Almquist and Wiksells, Stockholm, 1968;

S. Glashow, J. Iliopoulos, and L. Maiani, Phys. Rev. **D2**, 1285 (1970).

2. P.W. Higgs, Phys. Rev. Lett. **12**, 132 (1964);
idem, Phys. Rev. **145**, 1156 (1966);
F. Englert and R. Brout, Phys. Rev. Lett. **13**, 321 (1964);
G.S. Guralnik, C.R. Hagen, and T.W. Kibble, Phys. Rev. Lett. **13**, 585 (1964).
3. J. Wess and B. Zumino, Nucl. Phys. **B70**, 39 (1974); *idem*, Phys. Lett. **49B**, 52 (1974);
P. Fayet, Phys. Lett. **69B**, 489 (1977); *ibid.*, **84B**, 421 (1979); *ibid.*, **86B**, 272 (1979).
4. H.E. Haber and G.L. Kane, Phys. Rep. **C117** 75, (1985).
5. P.J. Franzini and P. Taxil, in *Z physics at LEP 1*, CERN 89-08 (1989).
6. Tevatron Higgs working group report, `hep-ph/0010338`.
7. ATLAS TDR on Physics performance, Vol. II, Chap. 19, *Higgs Bosons* (1999).
8. E. Accomando *et al.*, Physics Reports **299**, 1-78 (1998).
9. J.A. Aguilar-Saavedra *et al.*, TESLA Technical Design Report, Part III: *Physics at an e^+e^- Linear Collider*, `hep-ph/0106315`;
T. Abe *et al.*, SLAC-R-570 (2001), `hep-ph/0109166`;
M. Battaglia, `hep-ph/0103338`.
10. B. Autin, A. Blondel, and J. Ellis (eds.), CERN 99-02;
C.M. Ankenbrandt *et al.*, Phys. Rev. ST Acc. Beams **2**, 081001 (1999).
11. LEP Higgs Working Group, `http://lephiggs.web.cern.ch/LEPHIGGS/papers/index.html`.
12. J.F. Gunion *et al.*, *The Higgs Hunter's Guide* (Addison-Wesley) 1990.
13. H.E. Haber and M. Schmitt, *Supersymmetry*, in this volume.
14. N. Cabibbo *et al.*, Nucl. Phys. **B158**, 295 (1979);
G. Isidori, G. Ridolfi, and A. Strumia, Nucl. Phys. **B609**, 387 (2001).
15. T. Hambye and K. Riesselmann, Phys. Rev. **D55**, 7255 (1997).
16. C. Kolda and H. Murayama, JHEP **0007**, 035 (2000).
17. LEP Electroweak Working Group (July 2001), `http://lepewwg.web.cern.ch/LEPEWWG/`.
18. Y. Okada, M. Yamaguchi, and T. Yanagida, Theor. Phys. **85**, 1 (1991);
H. Haber and R. Hempfling, Phys. Lett. **66**, 1815 (1991);

J. Ellis, G. Ridolfi, and F. Zwirner, Phys. Lett. **B257**, 83 (1991);
M. Carena, M. Quiros, and C.E.M. Wagner, Nucl. Phys. **B461**, 407 (1996);
S. Heinemeyer, W. Hollik, and G. Weiglein, Phys. Lett. **B455**, 179 (1999); *idem*, Eur. Phys. J. **C9**, 343 (1999);
J.R. Espinosa and R.-J. Zhang, Nucl. Phys. **B586**, 3 (2000);
A. Brignole *et al.*, `hep-ph/0112177`.

19. M. Carena *et al.*, `hep-ph/9912223`.
20. M. Carena, S. Pokorski, and C. Wagner, Nucl. Phys. **B406**, 45 (1993);
V. Barger, M.S. Berger, and P. Ohmann, Phys. Rev. **D47**, 1093 (1993);
M. Carena and C. Wagner, Nucl. Phys. **B452**, 45 (1995).
21. J. Ellis, M.K. Gaillard, and D.V. Nanopoulos, Nucl. Phys. **B106**, 292 (1976);
B.L. Ioffe and V.A. Khoze, Sov. J. Part. Nucl. **9**, 50 (1978).
22. E. Gross, B.A. Kniehl, and G. Wolf, Z. Phys. **C63**, 417 (1994); erratum *ibid.*, **C66**, 32 (1995).
23. D.R.T. Jones and S.T. Petcov, Phys. Lett. **84B**, 440 (1979);
R.N. Cahn and S. Dawson, Phys. Lett. **136B**, 96 (1984); *ibid.*, **138B**, 464 (1984);
W. Kilian, M. Krämer, and P.M. Zerwas, Phys. Lett. **B373**, 135 (1996).
24. A. Djouadi, M. Spira, and P.M. Zerwas, Z. Phys. **C70**, 675 (1996).
25. S.L. Glashow, D.V. Nanopoulos, and A. Yildiz, Phys. Rev. **D18**, 1724 (1978);
A. Stange, W. Marciano, and S. Willenbrock, Phys. Rev. **D49**, 1354 (1994); *ibid.*, **D50** 4491, (1994).
26. A. Djouadi *et al.*, Z. Phys. **C70**, 435 (1996);
E. Ma, D.P. Roy, and J. Wudka, Phys. Rev. Lett. **80**, 1162 (1998).
27. P. Janot, *Searching for Higgs Bosons at LEP 1 and LEP 2*, in Perspectives in Higgs Physics II, World Scientific, ed. G.L. Kane (1998).
28. A.L. Read, in CERN Report 2000-005, p. 81 (2000);
T. Junk, Nucl. Inst. Meth. **A434**, 435 (1999).
29. Ref. [11], CERN-EP/98-046, 99-060, 2000-055;
Note for ICHEP'2000.
30. ALEPH Collab., Phys. Lett. **B495**, 1 (2000);

CERN-EP/2001-095, accepted for publication in Phys. Lett. **B** (2002).

31. DELPHI Collab., Phys. Lett. **B499**, 23 (2001);
L3 Collab., Phys. Lett. **B495**, 18 (2001); *ibid.*, **B517**, 319 (2001);
OPAL Collab., Phys. Lett. **B499**, 38 (2001).
32. LEP Higgs Working Group, CERN-EP/2001-055.
33. CDF Collab., Phys. Rev. Lett. **79**, 3819 (1997); *ibid.*, **81**, 5748 (1998).
34. DØ Collab., S. Abachi *et al.*, Fermilab-Conf-96/258-E.
35. D.E. Groom *et al.*, Eur. Phys. J. **C15**, 1 (2000).
36. DELPHI Collab., Phys. Lett. **B440**, 419 (1998);
OPAL Collab., Eur. Phys. J. **C7**, 407 (1999);
ALEPH Collab., Eur. Phys. J. **C17**, 223 (2000);
(*)DELPHI 2001-081 CONF 509.
37. Ref. [11], LHWG Note 2001-04.
38. CDF Collab., Phys. Rev. Lett. **86**, 472 (2001).
39. Ref. [11], LHWG Note/2001-05.
40. DØ Collab., Phys. Rev. Lett. **82**, 4975 (1999);
(*)FERMILAB-Conf-00-294-E.
41. CDF Collab., Phys. Rev. Lett. **79**, 357 (1997).
42. CDF Collab., Phys. Rev. **D62**, 012004 (2000).
43. J.A. Coarasa *et al.*, Phys. Lett. **B442**, 326 (1998);
J.A. Coarasa, J. Guasch, and J. Solá, `hep-ph/9903212`;
F.M. Borzumati and A. Djouadi, `hep-ph/9806301`.
44. P. Gambino and M. Misiak, Nucl. Phys. **B611**, 338 (2001): see Note added in proof.
45. R. Ellis *et al.*, Phys. Lett. **B179**, 119 (1986);
V. Barger, J. Hewett, and R, Phillips, Phys. Rev. **D41**, 3421 (1990).
46. S. Chen *et al.*, CLEO Collab., Phys. Rev. Lett. **87**, 251807 (2001);
G. Taylor, BELLE Collab., XXXVIth Rencontres de Moriond, March 2001;
ALEPH Collab., Phys. Lett. **B429**, 169 (1998).
47. ALEPH Collab., Phys. Lett. **B343**, 444 (1995);
DELPHI Collab., Z. Phys. **C72**, 207 (1996);
L3 Collab., Phys. Lett. **B317**, 637 (1993);
OPAL Collab., Eur. Phys. J. **C8**, 3 (1999).
48. Ref. [11], LHWG Note 2001-07.
49. OPAL Collab., Eur. Phys. J. **C18**, 425 (2001);
(*)DELPHI 2001-068 CONF 496.

50. (*)ALEPH PA13-027 (1996);
(*)DELPHI 99-76 CONF 263 (1999);
OPAL Collab., CERN-EP/2001-077, accepted for publication in Eur. Phys. J. **C** (2002).

51. G.B. Gelmini and M. Roncadelli, Phys. Lett. **B99**, 411 (1981);
R.N. Mohapatra and J.D. Vergados, Phys. Rev. Lett. **47**, 1713 (1981);
V. Barger *et al.*, Phys. Rev. **D26**, 218 (1982);
B. Dutta and R.N. Mohapatra, Phys. Rev. **D59**, 015018-1 (1999).

52. OPAL Collab., Phys. Lett. **B295**, 347 (1992);
CERN-EP/2001-082, accepted for publication in Phys. Lett. **B** (2002).

53. P. Fayet, Nucl. Phys. **B90**, 104 (1975);
S.F. King and P.L. White, Phys. Rev. **D53**, 4049 (1996).

54. (*)DELPHI 99-97 CONF 284.

55. Y. Chikashige, R.N. Mohapatra, and P.D. Peccei, Phys. Lett. **98B**, 265 (1981);
A.S. Joshipura and S.D. Rindani, Phys. Lett. **69**, 3269 (1992);
F. de Campos *et al.*, Phys. Rev. **D55**, 1316 (1997).

56. See Ref. 11, LHWG-Note/2001-06.

57. J. Ellis, M.K. Gaillard, and D.V. Nanopoulos, Nucl. Phys. **B106**, 292 (1976);
A. Abbasabadi *et al.*, Phys. Rev. **D52**, 3919 (1995);
R.N. Cahn, M.S. Chanowitz, and N. Fleishon, Phys. Lett. **B82**, 113 (1997).

58. G. Gamberini, G.F. Giudice, and G. Ridolfi, Nucl. Phys. **B292**, 237 (1987);
R. Bates, J.N. Ng, and P. Kalyniak, Phys. Rev. **D34**, 172 (1986);
K. Hagiwara, R. Szalapski, and D. Zeppenfeld, Phys. Lett. **B318**, 155 (1993);
O.J.P. Éboli *et al.*, Phys. Lett. **B434**, 340 (1998).

59. A.G. Akeroyd, Phys. Lett. **B368**, 89 (1996);
H.Haber, G. Kane, and T. Stirling, Nucl. Phys. **B161**, 93 (1979).

60. See Ref. 11, LHWG-Note/2001-08.

61. T. Affolder *et al.*, Phys. Rev. **D64**, 092002 (2001).

62. G.J. Gounaris, F. Renard, and D. Schildknecht, Phys. Lett. **B83**, 191 (1979);
V. Barger, T. Han, and R.J.N. Phillips, Phys. Rev. **D38**, 2766 (1988);

F. Boudjema and E. Chopin, Z. Phys. **C37**, 85 (1996);
A. Djouadi *et al.*, Eur. Phys. J. **C10**, 27 (1999).

63. B.W. Lee, C. Quigg, and H.B. Thacker, Phys. Rev. **D16**, 1519 (1977);
R.S. Chivukula *et al.*, `hep-ph/9503202`;
C. Yuan, `hep-ph/9712513`;
M. Chanowitz, `hep-ph/9812215`.

64. S. Weinberg, Phys. Rev. **D13**, 974 (1976); *ibid.*, **D19**, 1277 (1979);
L. Susskind, Phys. Rev. **D20**, 2619 (1979).